DESIGN AND RESEARCH ON THE CRUSHING SYSTEM OF THE TANK CLEANING ROBOT
/
贮罐清理机器人破碎系统的设计与研究

Yong TIAN[1)], Jian SONG[1)], Fuxiang XIE*[1)]
[1)] School of Machinery and Automation, Weifang University, Shandong/ China;
Tel: +86-18863637275 ; E-mail: 20210007@wfu.edu.cn
DOI: https://doi.org/10.35633/inmateh-74-27

Keywords: *Large tanks, robot, crushing system, EDEM, optimal operating parameters, crushing rate*

ABSTRACT
The existing equipment for cleaning large tanks has the problems of simple structure and single function. In order to solve this problem, a robot is designed to clean solid residues in tank, which integrates shoveling, crushing, sweeping and suction. And the crushing system of the robot is structurally designed and analyzed. Firstly, the crushing system is simulated and analyzed by using EDEM software. Then, the optimal operating parameters of the crushing device are determined by studying the effects of rotary knife pitch, rotary knife speed and rotary depth on the crushing rate. Finally, the crushing test is carried out on the cleaning robot, and the crushing rate is obtained as 83.6%, and the results show that the robot control system meets the design requirements. The study provides a certain reference for the research and development of the cleaning robot.

摘要
现有清理大型贮罐的装置结构简单、功能单一，为解决这一问题，以贮罐作为研究清理对象，提出了一种清理贮罐中固体残留物的机器人设计方案，研制了一种集铲装、破碎、清扫、吸尘为一体的清理装置，并对破碎装置进行了优化设计分析。使用EDEM 软件对机器人进行仿真分析，研究旋耕刀间距、旋耕刀转速和旋耕深度对破碎率的影响，分析确定了破碎装置的最优工作参数；通过对清理机器人进行性能试验，破碎试验得到破碎率为83.6%，该研究从结构设计到试验验证，为清理机器人的研究与发展提供了一定的参考。

INTRODUCTION

At present, there are two main cleaning methods for large storage tanks, one is to utilize a mechanical arm carrying a water spray device. The residue is flushed with the water spray device, and then the residue is stirred and mixed with the mechanical arm, and finally the mixture is extracted with the pump. Another way is to use the cleaning robot to clean up, the robot carries a crushing tool and high-pressure water spray device. The method is the use of high-pressure crushing device for residue crushing, and then the use of water jetting device for flushing, and finally the use of pumps to extract the mixture (*Li, 2021; Naser, 2015; Tan, 2021*).

In the 1980s, some developed countries began to research and design the storage tank cleaning device. Fig.1(a) shows the C-104NESL tracked folding vehicle (*Michal, 2012*), which has a folded width of 685 mm and an unfolded width of 1016 mm, with a front-mounted push shovel that can be used alone to concentrate the dried sludge in the tanks, and with nozzles and absorbers to work in conjunction with the push shovel in a remotely-controlled manner. Fig.1(b) shows the Industrobot cleaning robot developed by Offshore Cleaning systems in the United States, and Fig.1(c) shows the hydrotanker developed by Petroleum Ferment Company, which utilizes water jets to rinse the bottom of the tank (*Chen, 2019*). These two cleaning devices have a push shovel at the front and work in conjunction with the water jets above them, and are mainly used for cleaning large tanks.

Fig.1(d) shows the oil tank cleaning robot, which is an automated robot specialized in cleaning the residue at the bottom of the tank, with the functions of moving, adsorption and cleaning, and the cleaning methods mainly include water jet cleaning, mechanical force cleaning and ultrasonic cleaning (*Song, 2020*). Fig.1(e) shows a silt cleaning robot (*Nagatani et al., 2013*), which utilizes a forward device to feed the silt to the pump inlet, where it undergoes a rotating device to break up the debris, and then enters the silt transfer system. This device is mainly used for the cleaning of pools and urban pipelines. Fig.1(f) shows a multifunctional sweeper, which is a cleaning device integrating sweeping, vacuuming, sprinkling, mopping, recycling and transportation (*Naser, 2015*). The device is manually remote-controlled, the bottom of the car is equipped with a sweeping disk with a water spraying device and a sponge device used to absorb water, which is mainly used for roadway sweeping operations.

Fig.1(g) shows that the Chinese Academy of Sciences developed for nuclear power plant underwater operations, "underwater foreign body salvage robot" (*Lee et al., 2013*). The robot length is 420 mm, the width - 198 mm, the height - 236 mm and it can realize the underwater cleaning and salvage operations.

(a) C-104NESL (b) Industrobot (c) Hydrotanker

(d) Tank cleaning robot (e) Sludge removal robot (f) Multi-function sweeper (g) Recovery robot

Fig. 1 - Robotic arm cleaning device

Regarding the long-term residue in the storage tank, the cleaning effect is also greatly affected due to the complexity of the environment (*Grape, 2014; Mochizuki, 2014; Sawade, 2012; Zhong et al., 2015*). Therefore, designing a relevant cleaning device to solve these problems has important research significance and application value. This paper mainly focuses on the research and design of a cleaning device for solid residues in large storage tanks, and uses the software EDEM to simulate and analyze the crushing device, to study the effects of changes in the rotational speed, tilling depth and tillage knife spacing of the rotary blade on the crushing effect, and obtain the optimal combination of parameters.

MATERIALS AND METHODS

Design of Tank Cleaning Robot

The residual substances at the bottom of the tank mainly include slurries, salt cakes, or sediments, and have a certain hardness after prolonged storage (*Du et al., 2020; Liu et al., 2024*). Due to the small opening of the storage tank, there is consequent difficulty in removing the residuals at the bottom of the tank. In this paper, the overall structural design of the cleaning robot is carried out in consideration of the internal composition of the tank.

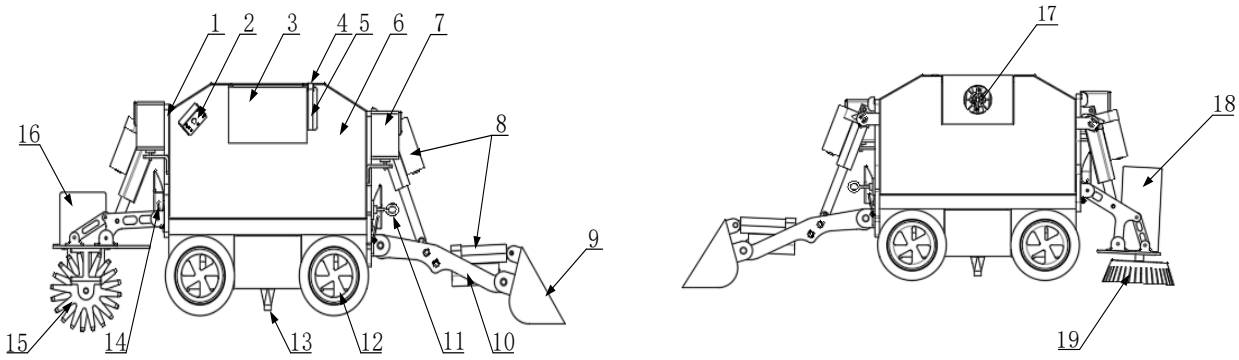

Fig. 2 - Structure of the cleaning robot

1-fixing plate, 2-camera, 3-dust collection box, 4-synchronous wheel, 5-synchronous belt, 6-main box, 7-searchlight, 8-electric actuator, 9-bucket, 10-linkage, 11-hooks, 12-rubber tires, 13-suction nozzle, 14-locking buckle, 15-rotary cutter, 16-protection shell of rotary motor, 17-fan, 18-protection illumination of sweeping motor, 19-brush plate

In view of the structural characteristics of nuclear storage tanks and the functions to be realized and requirements to be met, on the basis of ensuring the functionality, it is preferred to achieve the simplest structure and high stability, which is convenient for disassembly and replacement.

The overall structure is shown in Fig.2. The cleaning robot takes the vehicle body as the main body, and the front and rear suspensions are operated. The connection between the device modules and the vehicle body is fixed by latches to facilitate disassembly and replacement. Depending on the operation requirements, different device modules are hung. During the cleaning operation, the camera feeds back the situation in the storage tank to the ground display screen, and the robot is operated by the control box. Firstly, the residue or hard sediment is crushed by the crushing device, and then the disturbed residue is sent to the collection container by the shovel loading device. The fine particles are absorbed by the vacuum cleaning device, sucked into the dust collection box through the suction nozzles at the bottom of the vehicle, and finally the absorbed residue is poured into the collection container to complete the entire residue cleaning and collection work.

As an important part of the cleaning operation, the main function of the crushing is to use the designed mechanism to break the hard residue, so that the crushing device is more convenient and quicker to crush the residue into the collection container. The quality of its structural design has a significant impact on the crushing effect and working efficiency of the cleaning robot. The crushing scheme of rotary tillage blades has been adopted, using multiple disc rotary tillage blades as crushing tools. This scheme has the advantages of good disturbance resistance and high work efficiency for residues with low scab hardness. The specific rotary plowing crushing three-dimensional model is shown in Fig. 3.

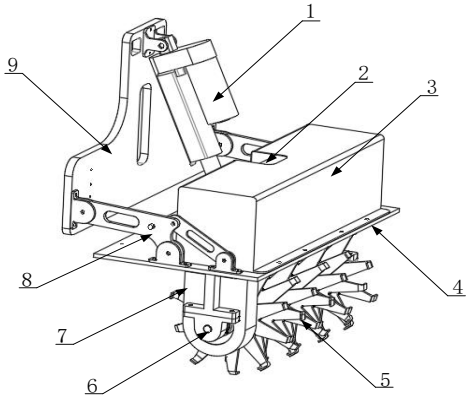

Fig. 3 - Three-dimensional diagram of rotary plowing and crushing device

1-lifting push rod, 2-motor, 3-motor shroud, 4-baffle plate, 5- rotary cutter, 6-bearing, 7-sprocket cover, 8-linkage, 9-fixing plate

RESULTS

Simulation Analysis of Crushing System

Crushing is an important part of the cleaning operation, and its main function is to break the hard residue using the designed mechanism. The setting of relevant parameters of the rotary blade has different effects on the crushing effect, and the influencing factors mainly include the tool spacing, rotary tillage depth, tool rotation speed and forward speed. In this paper, EDEM is used to simulate the crushing process of the rotary blade. During the simulation process, the simulation of residues and rotary tillage tools is achieved by calculating the forces on particles. Reasonable parameter settings and contact models to some extent determine the effectiveness of the simulation. The variation range of the forward speed is small, so it is not considered. A tool spacing of 10 mm to 20 mm is determined in the simulation, and the rotational speed of the rotary blade is set at 200 rpm to 350 rpm. In simulation, the radius of the particle model is usually set to 2 mm, 5 mm, and 10 mm (*Li et al., 2023; Zhu, 2016*). Based on the characteristics of the residue in the cleaned tank, the particle model radius is set to 2 mm, the bonding radius is set to 3 mm, and the rotary tiller simulation is shown in Fig.4.

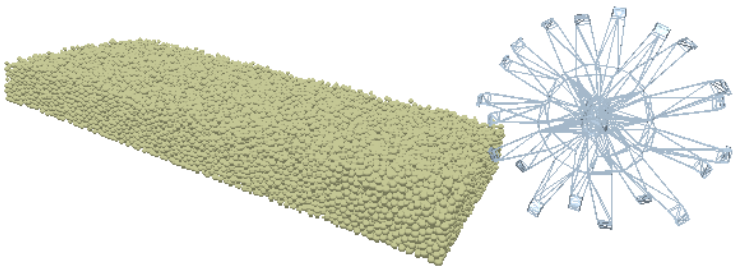

Fig. 4 - Analog simulation of rotary cutter

Breakage rate is an important manifestation of crushing effect. This article calculates the breakage rate by the number of bond breaks between particles. (*Yu, 2018*). The number of bond breaks between particles is statistically calculated by using post-processing Analyst in EDEM software, and then calculate the breakage rate by the given formula, which is expressed as follows:

$$I = \frac{N_b}{N_b + N_i} \times 100\% \quad (1)$$

where: I is the fragmentation rate, N_b is the number of broken particle bonds in the spinning zone, and N_i is the number of intact particle bonds in the spinning zone.

- Analysis of Orthogonal Tests

Taking the tool spacing, rotary tillage depth and tool speed as the influencing factors, and they are respectively marked as A, B, and C, and the breakage rate and forward resistance are taken as the response values, -1, 0, and 1 are respectively the low, medium, and high levels, and a three-factor three-level Box-Behnken test is established.

Applying the Box-Behnken response surface design principle, a total of 17 test points are designed in the experiment to evaluate and calculate the experimental error (*Sun et al., 2023*), and the Box-Behnken response surface test results and analysis are obtained, as shown Table 2.

Table 1

Box-Behnken test factor level table

Factor code		Experimental factors		Level
		Low-level -1	Mid-level 0	High-level 1
A	Tool spacing（mm）	10	15	20
B	Rotary depth（mm）	20	30	40
C	Tool speed（rpm）	150	200	250

Table 2

Box-Behnken Response Surface Test

Serial No.	Tool spacing (mm)	Rotary depth (mm)	Tool speed (rpm)	Horizontal resistance (N)	Crushing rate (%)
1	10.00	30.00	150.00	5.80	83.48
2	20.00	20.00	200.00	5.82	82.59
3	15.00	30.00	200.00	5.89	86.24
4	15.00	30.00	200.00	5.71	86.45
5	20.00	40.00	200.00	7.91	88.05
6	15.00	30.00	200.00	5.82	86.40
7	10.00	30.00	250.00	5.90	88.03
8	20.00	30.00	150.00	5.89	82.16
9	15.00	30.00	200.00	5.75	86.35
10	10.00	40.00	250.00	7.54	90.68
11	15.00	30.00	200.00	5.91	86.32
12	15.00	40.00	150.00	7.86	85.93
13	15.00	20.00	250.00	6.25	84.36
14	10.00	20.00	200.00	5.60	81.53
15	20.00	30.00	250.00	6.30	88.84
16	10.00	40.00	200.00	6.84	89.44
17	15.00	20.00	150.00	5.24	78.33

- Analysis of the Effect of Factors on Horizontal Resistance

The variance of horizontal resistance was analyzed using Design-Expert V8.0.6 software and the results are shown in Table 3. From the results of the analysis in Table 3, it can be seen that the *P* value of the horizontal resistance regression model is less than 0.001, indicating that the regression model is significant. The value of P of the misfit term is 0.0708, which is greater than 0.05, so the misfit term is not significant, indicating that the model is more reliable. The P-value shows that rotary tillage depth *B* has a more significant effect on horizontal resistance, tool spacing A has the second most significant effect on horizontal resistance, and tool speed *C* has a non-significant effect on horizontal resistance. After analyzing, it can be seen that the order of influence of the three factors on horizontal resistance is *B*>*A*>*C*, i.e., tool depth>tool spacing>tool speed. Among them, the interaction term BC has a very significant effect (P<0.001) and *AB* has a significant effect (P<0.01). The secondary term B^2 had a highly significant (P<0.001) effect on the results.

Table 3

Analysis of Variance for Horizontal Resistance

Source	square sum	DOF	mean square	F	P	significance
model	9.95	9	1.11	52.10	<0.0001	***
A	0.40	1	0.40	18.67	0.0035	**
B	6.37	1	6.37	300.34	<0.0001	***
C	0.21	1	0.21	9.96	0.0160	*
AB	0.18	1	0.18	8.51	0.0224	*
AC	0.024	1	0.024	1.13	0.3226	
BC	0.38	1	0.38	17.83	0.0039	**
A^2	2.368e-06	1	2.368e-06	1.116e-04	0.9919	
B^2	2.22	1	2.22	104.53	<0.0001	***
C^2	0.10	1	0.10	4.81	0.0643	
residual	0.15	7	0.021			
lost proposal	0.12	3	0.040	5.29	0.0708	
pure error	0.030	4	7.48e-03			
sum	10.10	16				

*Note: * indicates p<0.05 (significant); ** indicates p<0.01 (highly significant); *** indicates p<0.001 (highly significant).*

In order to better analyze the effect of the test factors on the horizontal resistance, choose one of the three test factors to be fixed as the zero level, choose the other two factors to observe the effect on the crushing rate, and use the response surface generated in the software to observe the size of the effect of each factor on the horizontal resistance.

As shown in Fig. 5, it can be seen that the depth of rotary tillage has a significant impact on the horizontal resistance of the cutting tool, and the effect of rotary tillage depth on the horizontal resistance of the cutting tool is more significant than the effect of tool spacing.

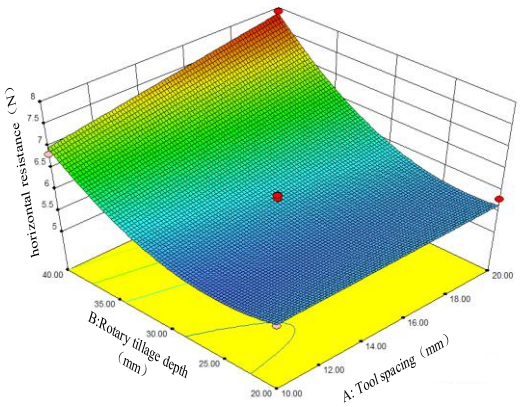

(a) tool spacing

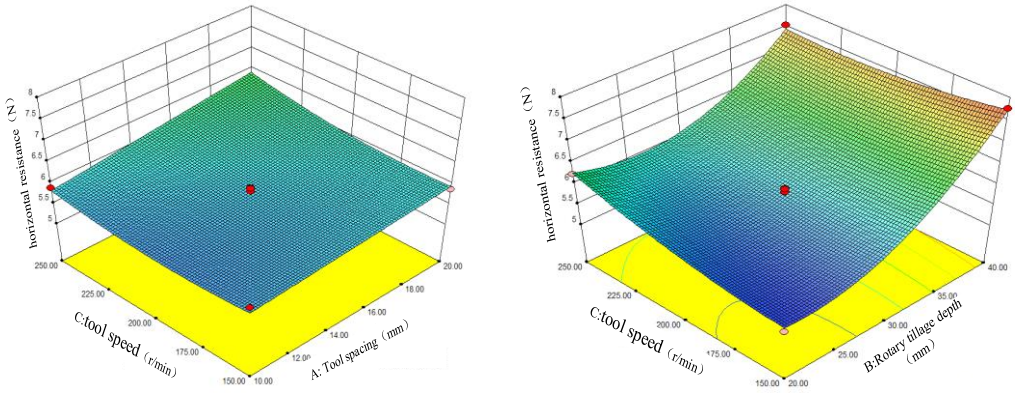

(b) tool speed (c) rotary tillage depth

Fig. 5 - Response surface on tool horizontal resistance

For rotary tillage depths between 20 mm and 30 mm, the increase in horizontal resistance is small, while for rotary tillage depths greater than 30 mm, the increase is significant. The tool speed and tool spacing have no significant effect on the horizontal resistance of the tool, and the horizontal resistance experienced by the tool does not change significantly with changes in tool speed and tool spacing.

- Analysis of the effect of factors on crushing rate

Table 4

Analysis of Variance for Crushing Rate

Source	square sum	DOF	mean square	F	P	significance
model	162.17	9	18.02	1361.31	<0.0001	***
A	0.088	1	0.088	6.66	0.0364	*
B	93.09	1	93.09	7033.09	<0.0001	***
C	60.56	1	60.56	4574.88	<0.0001	***
AB	1.50	1	1.50	113.37	<0.0001	***
AC	1.13	1	1.13	85.69	<0.0001	***
BC	0.41	1	0.41	30.94	<0.0008	***
A^2	0.023	1	0.023	1.72	0.2313	
B^2	3.23	1	3.23	244.10	<0.0001	***
C^2	1.78	1	1.78	134.81	<0.0001	***
residual	0.093	7	0.013			
lost proposal	0.067	3	0.022	3.52	0.1280	
pure error	0.025	4	6.370E-003			
sum	162.26	16				

*Note: * indicates p<0.05 (significant); ** indicates p<0.01 (highly significant); *** indicates p<0.001 (highly significant).*

As can be seen from the results of the analysis in Table 4, the regression model is significant, and the lost proposal is not significant, indicating that the model is relatively reliable. From the P-value, it can be seen that B and C have a significant impact on horizontal resistance. After analysis, it can be seen that the three factors on horizontal resistance are in the order of *C*>*B*>*A*, that is, tool speed>rotary plowing depth>tool spacing. Among them, the interaction terms *AB, AC* and *BC* had highly significant effects (P<0.001). The secondary terms B^2 and C^2 had highly significant (P<0.001) effect on the results. A^2 had no significant effect on the results. Use software to generate corresponding response surfaces and intuitively study the impact of various factors on the fragmentation rate, as shown in Fig.6.

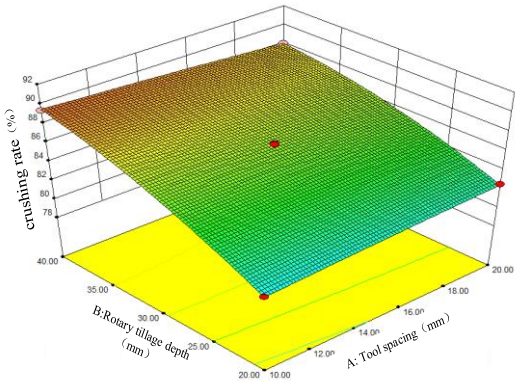

(a) tool spacing

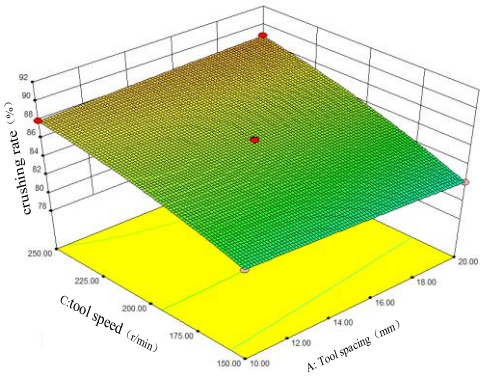

(b) tool speed

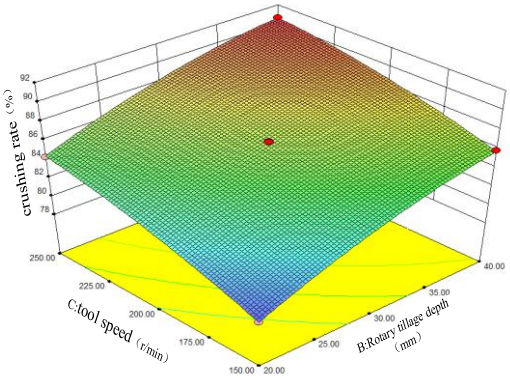

(c) rotary tillage depth

Fig. 6 - Response surface on fragmentation rate

- Parameter Optimization

The purpose of parameter optimization is to ensure that the crushing device can obtain better crushing effect and smaller horizontal resistance within the scope of meeting the operational indexes. Taking the horizontal resistance y_1 and the crushing rate y_2 as the function of the test indexes, the optimal combination of the tool spacing A, the tool rotational speed B and the rotary tillage depth C is selected, analyzed and solved by using Design-Expert with the objective function and constraints as follows:
Objective function:

$$\begin{cases} y_1(A、\ B、\ C) \to \max \\ y_2(A、\ B、\ C) \to \min \end{cases} \tag{2}$$

Constraints:

$$s.t. \begin{cases} 10 \le A \le 20 \\ 20 \le B \le 40 \\ 150 \le C \le 250 \end{cases} \tag{3}$$

It can be seen through simulation that the optimal combination of parameters for the designed crushing device is determined in the case of satisfying the constraints and the objective function tool spacing of 10 mm, rotary depth of 30 mm, tool speed of 230 rpm, horizontal resistance of 5.8 N, and a crushing rate of 88.30%, according to the optimal combination of the measured parameters applied to the actual crushing operation.

Prototype Development and Testing

To verify the feasibility of the tank cleaning robot, a site that meets the requirements of the project party was selected for testing, and the crushing rate was used as the main verification indicator for the experiment:

$$E = \frac{G_s - G_a}{G_s} \times 100\% \quad (4)$$

where: E for the crushing rate; G_a for the mass of the pieces less than 4 cm in the crushing zone; G_s for the total mass of the material in the crushing zone. And five 0.2 m*0.2 m boxes were homemade, and the mass of all the soil in the tillage layer in the boxes and the clods of soil with the longest side less than 4 cm were weighed (*Yu, 2021*). The experimental results are shown in Fig.7.

Fig. 7 - Sample machine test

The traveling speed was set to 0.1 m/s, 0.2 m/s, 0.3 m/s, 0.4 m/s, the tool spacing was 10 mm, the tool speed was set to 230 rpm, and the depth of rotary tillage was 30 mm. Through the experimental comparisons under different advancing speeds, the crushing rate under the optimal parameters obtained from the simulation was tested. The results were analyzed and the data were obtained.

As can be seen from Table 5, when the traveling speed is 0.1m/s, the highest crushing rate is 83.6%, and when the traveling speed is 0.4 m/s, the lowest crushing rate is 74.2%. Through the value of speed and crushing rate analysis, in the value range of the higher speed crushing rate gradually decreased, when the traveling speed of 0.1 m/s crushing device in the low-speed operation is closer to the simulation results, the device is more suitable for low-speed operation under the use of simulation parameters.

Table 5

Comparison of Crushing Rate Tests

Travel speed (m/s)	Crushing rate E (%)					
	test1	test 2	test 3	test 4	test 5	average value
0.1	86	83	80	85	81	83.6
0.2	81	82	80	83	79	81
0.3	83	73	81	75	73	77
0.4	72	76	78	70	75	74.2

CONCLUSIONS

In this article, EDEM software is used to simulate the fragmentation of rotary tillage equipment. By selecting a reasonable particle contact model, the rotary tillage blade is simulated. The blade spacing, blade speed, and rotary tillage depth are used as experimental factors, and horizontal resistance and fragmentation rate are used as experimental indicators to study the effects of the three experimental factors on the experimental indicators. By analyzing the regression equation and response surface, the significance of each experimental factor on the experimental indicators was determined. And through parameter optimization, the optimal parameter combination was obtained. Finally, based on the optimized simulation parameters, an experiment was conducted and a crushing rate of 83.6% was obtained at a speed of 0.1 m/s. The error between the experimental data and the simulation data was relatively small.

ACKNOWLEDGEMENT

This research has received support from the Weifang Science and technology development plan project (2022GX005).

REFERENCES

[1] Chen L., (2019). *Design of explosion-proof cleaning robot system for residual oil at the bottom of horizontal tanker (卧式油罐车罐底残油防爆型清理机器人系统设计).* Master dissertation, Anhui University of Technology, Anhui/China.

[2] Du, J., Zhang, W., Zhu, Y., (2020). Characterization of power distribution of rotary buried knife roller based on discrete element method (基于离散元法的旋埋刀辊功率分配特性研究). *Journal of Anhui Agricultural University*, Vol. 47, pp. 1031-1037, Anhui/China.

[3] Grape, S., Svaerd, S., Hellesen, C., Jansson, P., & Lindell, M., (2014). New perspectives on nuclear power—generation iv nuclear energy systems to strengthen nuclear non-proliferation and support nuclear disarmament. *Energy Policy*, Vol. 73, pp. 815-819, England.

[4] Lee, W., Hirai, M., & Hirose, S., (2013). Gunryu iii: reconfigurable magnetic wall-climbing robot for decommissioning of nuclear reactor. *Advanced Robotics*, Vol. 27, pp. 1099-1111, Japan.

[5] Li, X., (2021). *Intermediate level liquid radwaste tank decommissioning technological plan design (中放废液贮罐退役工艺方案设计)*. Master dissertation, University of South China, Guangdong/China.

[6] Li, S., Diao, P., Zhao, Y., Miao, H., Li, X., & Zhao, H., (2023). Calibration of discrete element parameters for soil in high-speed tillage (高速耕作条件下土壤离散元参数标定). *INMATEH - Agricultural Engineering*, Vol. 71, pp. 248-258, Romania.

[7] Liu, Z., Shang, S., Ma, S.,Hou, Y., Dong, T., & He, X., (2024). Optimization by coupled RecurDyn-EDEM simulation: Optimization tests of a three-stage low-loss separation device for potato soil (RecurDyn-EDEM 耦合仿真优化: 三段式薯土低损分离装置优化试验). *INMATEH - Agricultural Engineering*, Vol. 72, pp. 138-147, Romania.

[8] Michal, V., (2012). Remote operation and robotics technologies in nuclear decommissioning projects – ScienceDirect. *Nuclear Decommissioning*, pp. 346-374.

[9] Mochizuki, M., Singh, R., Nguyen, T., & Nguyen, T., (2014). Heat pipe based passive emergency core cooling system for safe shutdown of nuclear power reactor. *Applied Thermal Engineering*, Vol. 73, pp. 699-706, England.

[10] Nagatani, K., Kiribayashi, S., Okada, Y., Otake, K., Yoshida, K., & Tadokoro, S., (2013). Emergency response to the nuclear accident at the Fukushima Daiichi Nuclear Power Plants using mobile rescue robots. *Journal of Field Robotics*, Vol. 30, pp. 44-63, USA.

[11] Naser, H., (2015). Analysing the long-run relationship among oil market, nuclear energy consumption, and economic growth: an evidence from emerging economies. *Energy*, Vol. 89, pp. 421-434, England.

[12] Sawade, C., Turnock, S., Forrester, A., & Toward, M., (2012). Improved rehabilitation and training techniques through the use of motion simulation – core strength conditioning for elite rowers – ScienceDirect. *Procedia Engineering*, Vol. 34, pp. 646-651, Netherland.

[13] Song Z., Zhou C., Zhang S., (2020). Application of dredging robot in culvert dredging project (清淤机器人在暗涵疏浚工程中的应用). *Northwest Hydropower*, Vol. 1, pp. 70-73, Shanxi/China.

[14] Sun, J., Yang, L., Xu, B., & Guo, Y., (2023). Design and experiment of a single-row small grain precision seeder (单行小籽粒精少量播种机设计与试验). *INMATEH - Agricultural Engineering*, Vol. 70, pp. 127-136, Romania.

[15] Tan, X., (2021). Analyzing Chinese nuclear energy development situation and outlook (浅析中国核能发展状况及展望). *China Plant Engineering*, Vol. 19, pp. 235-236, Beijing/China.

[16] Yu, C., (2018). Development and test of straw pulling mechanism of mobile tobacco straw pulling and crushing machine (移动式烟秆拔秆破碎机拔秆机构的研制及试验). Master dissertation, Guizhou University, Guizhou/China.

[17] Yu, C., (2021). Construction and validation of a multi-phase coupled simulation model of knife roller-straw-soil (刀辊-麦秆-土壤多相耦合仿真模型构建及验证). Master dissertation, Anhui Agricultural University, Anhui/China.

[18] Zhong, Y., Z., Fu, Y., Gao, P., (2015). Retrieval methods and techniques for tank storaged HLLW (槽贮高放废物回取方法和技术). *Guangdong Chemical Industry*, Vol.1, pp. 13-14, Guangdong/China.

[19] Zhu, H., (2016). Simulation and experimental research on furrowing working parts of no-tillage fertilizer planter (免耕施肥播种机开沟工作部件仿真与试验研究). Master dissertation, South China Agricultural University, Guangdong/China.